CSIRO PUBLISHING

www.publish.csiro.au/journals/rfd *Reproduction, Fertility and Development*, 2006, **18**, 559–571

Nuclear magnetic resonance spectroscopy of bovine ovarian follicular fluid at four selected times of the oestrous cycle

Gordon E. Sarty[A,B,E], *Edward J. Kendall*[B], *Gregg P. Adams*[C] *and Roger A. Pierson*[D]

[A]Department of Psychology, College of Arts and Science, University of Saskatchewan, Saskatoon, Saskatchewan, Canada.
[B]Department of Medical Imaging, College of Medicine, University of Saskatchewan, Saskatoon, Saskatchewan, Canada.
[C]Department of Veterinary Medical Biosciences, Western College of Veterinary Medicine, University of Saskatchewan, Saskatoon, Saskatchewan, Canada.
[D]Department of Obstetrics, Gynaecology and Reproductive Sciences, College of Medicine, University of Saskatchewan, Saskatoon, Saskatchewan, Canada.
[E]Corresponding author. Email: gordon.sarty@usask.ca

Abstract. The objective of the study was to determine if nuclear magnetic resonance (NMR) spectral features of ovarian follicular fluid were correlated with the physiological status of follicles so that we could assess the feasibility of using NMR spectroscopy during assisted reproduction therapy. Thirty-five sexually mature, nullparious heifers were monitored by transrectal ultrasonography to assess their follicle wave status during the oestrous cycle. Ovariectomies were performed on Day 3 of wave 1 (D3W1, $n = 10$), Day 6 of wave 1 (D6W1, $n = 9$), Day 1 of wave 2 (D1W2, $n = 9$), or in the immediate preovulatory period of at least 17 days after ovulation ($D \geq 17$, $n = 9$). Follicle status was determined to be dominant or subordinate. Follicular fluid was extracted from the follicles and NMR spectra were collected. Principal components were extracted from ratios of line amplitudes and tested for effects of follicle status (dominant *v.* subordinate) and cycle time point (D1W3, D1W6, D1W2 and $D \geq 17$) using multivariate analysis of variance. For most line ratio combinations, main effects of status, time point and their interaction were found ($P < 0.05$). We concluded that NMR spectra may be used for the determination of ovarian follicle physiological status.

Extra keywords: assisted reproduction technology, bovine, follicle, ovary, spectroscopy.

Introduction

Success in assisted reproduction technology (ART), for both humans and animals, depends on several decisions made throughout the course of therapy. Better decisions can be made with more available information and the probability of pregnancy as an outcome becomes higher. Nuclear magnetic resonance spectroscopy may be a useful means of obtaining additional information about the physiological status of an ovarian follicle (Gérard *et al*. 2002). Specifically, knowledge of whether a dominant follicle is destined to atresia or may continue on to ovulation would represent an important advance in our ability to predict ART outcomes and tailor clinical protocols to the needs of individual women.

Ovarian follicles undergo many physiological changes during the recruitment, selection and, finally, dominance or regression phases of folliculogenesis. It has been recently demonstrated that women undergo either two or three waves of follicular development during the menstrual cycle, similar to the wave patterns of folliculogenesis observed in domestic animal species, most notably horses and cows (Adams and Pierson 1995; Baerwald *et al*. 2003*a*, 2003*b*; Ginther *et al*. 2004). There has been no previous model system with which to perform experiments that are ethically problematic in humans. Therefore, we wished to further the exploration of the bovine model for human folliculogenesis.

In a previously reported magnetic resonance imaging (MRI) study, bovine ovaries were resected at four physiologically critical time points in the oestrous cycle (Hilton *et al*. 2000, 2001, 2003). For the present study, we obtained nuclear magnetic resonance (NMR) spectra of ovarian follicular fluid from the same ovaries at the conclusion of the imaging. Our objective was to test the hypothesis that changes in the NMR spectra of the follicular fluid would reflect the physiological status of the follicle. We wished to determine if an NMR approach to exploring follicular physiology was warranted before initiating an *in vivo* study to examine animal and, ultimately, human folliculogenesis using proton NMR spectroscopy of extracted follicular fluid.

 10.1071/RD06010 1031-3613/06/050559

Materials and methods

Animal selection

The procedures for the assignment of animals to the ovariectomy groups, ultrasonography and ovariectomies were previously described by Singh *et al*. (1997). The animals and the ovaries from which the follicular fluid was extracted for the present analysis were identical to those of the ovarian MRI studies described by Hilton *et al*. (2000, 2001, 2003). The study was conducted in accordance with guidelines for the ethical use of animals in research outlined by the Canadian Council of Animal Care and was approved by the University of Saskatchewan Institutional Review Board.

Briefly, ovarian development in 35 sexually mature (16–18 months old), nullparious crossbred (primarily Hereford) heifers was monitored by daily transrectal ultrasonography using a 7.5-MHz, linear-array transducer (Aloka SSD 500, ISM, Edmonton, AB, Canada) to monitor the development of ovarian follicles of 4-mm diameter, or larger, for the experimental period. On average, the ovaries were $3 \times 2.25 \times 2.25$ cm in dimension, with ovaries early in the cycle being smaller and ovaries with a mature corpus luteum and a 20-mm dominant follicle being somewhat larger. Hand-drawn diagrams (maps) showing the spatial location and diameter of individual follicles and corpora lutea were used to determine the day of follicle growth wave emergence (Day 0). The day of wave emergence was defined as the day at which the dominant follicle, which was defined as the largest follicle of the wave, was first detected at a diameter of 4–5 mm. Follicles in the wave smaller than the dominant follicle were labelled subordinate follicles.

All cows exhibited two waves of follicular growth per oestrous cycle in which the dominant follicle of the first wave became atretic as a second growth wave of follicles emerged. The dominant follicle of the second wave generally ovulates. Heifers were randomly designated for ovariectomy on Day 3 of wave 1 (D3W1, $n = 10$), Day 6 of wave 1 (D6W1, $n = 9$), Day 1 of wave 2 (D1W2, $n = 9$), or in the immediate preovulatory period of at least 17 days after ovulation ($D \geq 17$, $n = 9$). On D1W2, the largest follicle not of wave 1 was designated as the dominant follicle. The time for the $D \geq 17$ ovariectomy was 1 day after the detection of pro-oestrus. The days (groups) of ovariectomy were presumed to represent the growing (D1W3), early static (D6W1), late static (D1W2) and regressing phases ($D \geq 17$) of the larger wave 1 follicles as well as the preselection (D1W2) phase and the post-selection growing phase ($D \geq 17$) of the preovulatory dominant follicle of wave 2.

Ovaries were removed from the heifers through a single incision through the dorsolateral aspect of the vaginal wall (Hudson 1986). Surgery was conducted with cows in the standing position and under caudal epidural anaesthesia according to Canadian standards of good clinical practice. Immediately after ovariectomy, ovaries were placed in warm (37°C) physiological saline and transported to the MRI suite. The ovaries were removed from the saline ~60 min after ovariectomy and imaged for approximately another 60 min (Hilton *et al*. 2000, 2001, 2003). After imaging, the follicular fluid was aspirated from the dominant follicle, from the first subordinate follicle and from the remaining subordinate follicles, whose fluid were pooled in order to obtain a sample size similar to the large follicles. Follicular fluid was classified into two categories: (*1*) fluid from the dominant (largest) follicle; and (*2*) fluid from the subordinate follicles. No distinction was made between the first subordinate follicle and the pooled remaining follicles. After aspiration, the follicular fluid was frozen at −12°C until NMR spectroscopy was performed approximately 1 month later.

Nuclear magnetic resonance spectroscopy

Samples were thawed and mixed with 0.5 mL of $CDCl_3$ in a 5 mm (OD) borosilicate NMR sample tube (Wilmad, Buena, NJ, USA). Samples were maintained at room temperature for the duration of the experiment (8 h), during which the spectra were monitored to confirm their stability.

Proton spectroscopy was performed on a Bruker AMX500 (11.7T) spectrometer (Rheinstetten, Germany) equipped with a probe dual tuned for ^{1}H and ^{13}C. Signal was acquired into 32 768 points using a one-pulse experiment with $T_R = 2$ s, a 90° pulse and a receiver bandwidth of 8475 Hz. One hundred and twenty averages were collected for a total acquisition time of 4 min. Data were processed using exponential multiplication resulting in a frequency resolution of 0.56 Hz and a line broadening of 0.3 Hz. All spectra were manually phased and baseline corrected before peak quantification.

In addition to examining the chemical composition of the follicular fluid, the influence of the stage of the oestrous cycle on the fluid's physical properties was investigated. The T_1 relaxation time, a potential measure of viscosity, was determined for the lactate doublet (1.34 p.p.m.) using an inversion recovery sequence. Inversion times $T_I = 50$, 500, 2000, 5000 and 10 000 ms were used to sample the relaxation curve. The relaxation coefficient was calculated by fitting the signal intensities, S_I, obtained at each T_I to:

$$S_I = S_0(1 - 2\exp[-T_I/T_1]) \quad (1)$$

where S_0 is the equilibrium value. Other acquisition conditions were as above for the proton spectroscopy. The lactate doublet arises from the interaction between the CH_3 protons and the CH moiety of the lactate molecule. Each of the protons on the CH_3 are chemically equivalent and exhibit an identical chemical shift. However, the time-averaged interaction with the CH reflects the additive effect of the two spin states. As a result of this interaction, (u + d or u + u), the signal is split and resonates as a doublet. The time course of interaction is fast compared with the relaxation rate and the spin population remains chemically identical. As a result, each of the doublets are expected to have the same relaxation properties (ignoring the very minor effects of field augmentation on relaxation rate).

Spectral peaks were identified using the tables of Pretsch *et al.* (2000) and using previously published NMR spectra of mare ovarian follicular fluid (Gérard *et al*. 2002). The appearance of spectral peaks in expected locations, especially the lactate doublet, confirmed that there was no significant chemical shift introduced by the addition of $CDCl_3$ to the samples.

Data analysis

Three types of analyses were applied to the spectral data. The first was an analysis of the lactate peak T_1 relaxation rates. The remaining two analyses were of ratios of spectral line amplitudes (spectral peak heights): one analysis contained the lactate peaks and the other did not contain the lactate peaks. The lactate peaks were excluded from one of the line ratio analyses because the presence of lactate was likely caused by cell death and may have obscured the variation of the other peaks with the given factors. Spectral line amplitudes were quantified from the processed NMR spectra using the NUTS NMR Data Processing Software (Acorn NMR, Livermore, CA, USA).

For the analysis of the lactate peak relaxation rates, the two factors of time point of ovariectomy and follicle physiological status (T and S, see below) were combined into one factor with eight levels and a second factor for the high-frequency *v.* low-frequency peak. A two-way multivariate analysis of variance (MANOVA) was applied to determine if significant omnibus differences existed between the levels, and was followed by multiple pairwise comparisons for each of the high- and low-frequency peaks, using least significant differences (no *P*-value correction for multiple comparisons).

The ratios of lines that could be identified in every case were analysed for both line ratio analyses (with and without lactate). The data were grouped by two factors. The first factor was T (time point of ovariectomy), which consisted of four levels: Day 3 of wave 1 (D3W1), Day 6 of wave 1 (D6W1), Day 1 of wave 2 (D1W2), and the immediate preovulatory period of at least 17 days after ovulation ($D \geq 17$). The second

factor was S (follicle physiological status), which was either dominant (largest of the current wave) or subordinate. A separate analysis was done using each line amplitude, in turn, as the denominator. For each analysis, a principal components analysis was completed and components having an eigenvalue greater than 1 were used for subsequent MANOVA analysis. The cutoff of 1 for the eigenvalue ensured that the information contained in each retained component was equal to the information contained in one or more of the line ratios. An individual principal component identifies linear combinations of components that vary together. Between two and four relevant principal components were found in each case. The retained principal components were then subjected to a two-way MANOVA. Main effects and interactions were identified and profile plots were produced. Multiple comparisons beyond the MANOVAs were not attempted owing to the high number of tests done with the ratios.

Results

A typical ovarian follicular fluid spectrum, showing features observed in all of our collected spectra, is shown in Fig. 1. Eleven peaks were identified in all samples. The peaks corresponded to lactate (two peaks), alanine (two peaks), acetate, creatine and three unknown sources, U1, U2 (2 peaks) and U4 (2 peaks). Progesterone (or at least peaks in the region where progesterone would be expected) was detected in several samples, but not in all samples. Setting the progesterone amplitude to zero for samples in which progesterone was not detected and computing a univariate two-way analysis of variance, with factors T (time point of ovariectomy) and S (follicle physiological status – see Materials and methods), did not show any significant ($\alpha = 0.05$) variation with these factors.

Lactate T_1

Results of the lactate T_1 analysis are shown in Fig. 2. The amplitudes of the twin lactate peaks varied similarly across the groups, as expected. The omnibus multivariate analysis of variance (MANOVA) revealed that overall differences between groups was marginal ($P = 0.073$ based on Roy's largest root (Rencher 1998)). Nevertheless, independent pairwise comparisons for each of the high- and low-frequency peaks were made because the MANOVA treats the two frequencies as a vector and does not directly compare the scalar values. For both peaks, consistent differences were found between the lactate peak amplitudes for the dominant and subordinate groups at D1W2 ($P = 0.021$, low frequency (lf), $P = 0.037$, high frequency (hf)) and between the subordinate follicles at D6W1 and dominant follicles at D1W2 ($P = 0.008$, lf, $P = 0.018$, hf). The other differences found were as follows: dominant at D6W1 and dominant at D1W2 ($P = 0.050$, lf), subordinate at D6W1 and subordinate at D ≥ 17 ($P = 0.019$, lf) and, subordinate at D3W1 and dominant at D1W2 ($P = 0.025$, hf).

Line ratios

The distribution of the retained (eigenvalues greater than 1) principal components for line ratio combinations that exclude the lactate lines is given in Table 1 and the combinations that include the lactate lines are given in Table 2. In most cases, the principal components have nearly equal, and large (close to 1), contributions from all line ratios, which indicates that, relative to the given denominator line, all the lines varied essentially in unison.

Profile plots with respect to the T and S grouping variables for line ratio combinations that exclude the lactate lines are given in Figs 3–5. Profile plots with respect to the T and S grouping variables for line ratio combinations

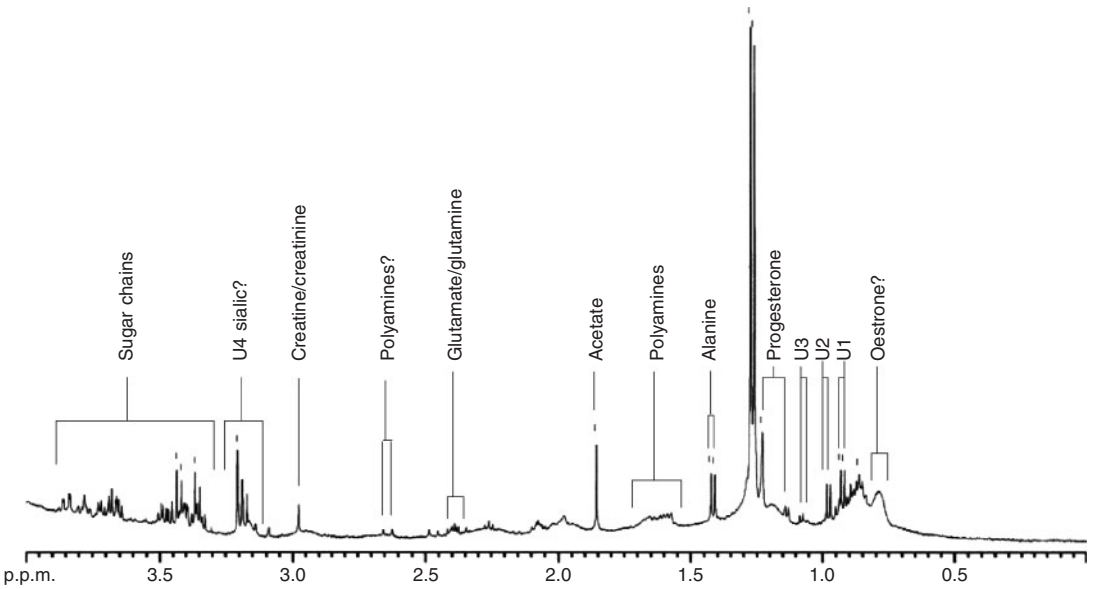

Fig. 1. ^{1}H NMR spectrum of follicular fluid showing the non-aromatic portion of the spectrum. The tall twin peak is lactate.

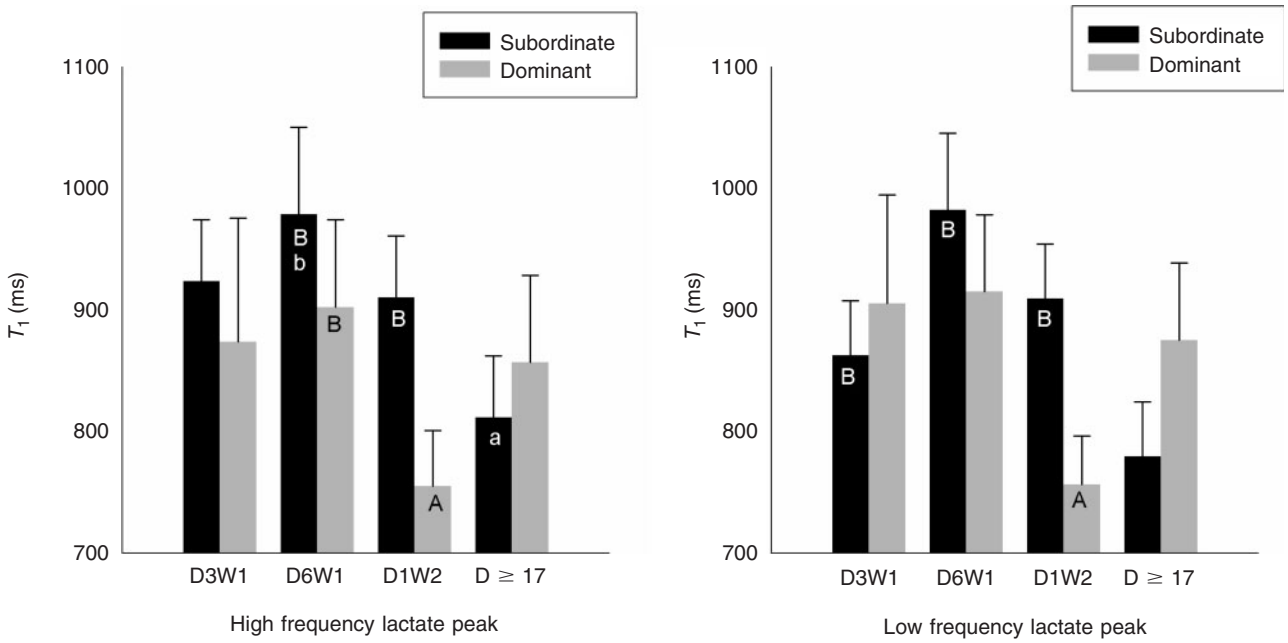

Fig. 2. Summary of T_1 measurements at the frequencies of the twin lactate peaks. Values labelled with 'A' differ from values labelled with 'B'. Similarly, values labelled with 'a' differ from values labelled with 'b'. ($P < 0.05$ in all cases.) Data are displayed as mean with s.e.m.

Table 1. Principal component directions – lactate not considered
l_d, line denominator; c, principal component number; λ, eigenvalue

l_d	c	λ	U1-2	U2-1	U2-2	Alanine-1	Alanine-2	Acetate	Creatine	U4-3	U4-4
U1-2	1	4.7	–	0.723	0.818	0.783	0.783	0.569	0.801	0.788	0.808
	2	1.4	–	0.537	0.443	−0.461	−0.439	0.566	−0.407	0.157	−0.204
	3	1.1	–	0.256	0.188	0.404	0.421	0.068	−0.218	−0.539	−0.525
U2-1	1	4.0	0.552	–	0.696	0.848	0.843	0.121	0.837	0.629	0.803
	2	1.6	−0.557	–	−0.261	−0.327	−0.344	0.542	0.234	0.648	0.482
	3	1.1	0.481	–	0.592	−0.293	−0.275	0.444	−0.330	0.196	−0.122
U2-2	1	3.2	−0.076	−0.291	–	0.782	0.768	0.037	0.909	0.587	0.843
	2	1.9	0.620	0.050	–	0.535	0.543	−0.578	−0.031	−0.684	−0.382
	3	1.1	−0.346	0.577	–	0.269	0.261	0.604	0.045	−0.235	−0.233
Alanine-1	1	3.3	0.723	0.827	0.867	–	−0.154	0.573	0.461	0.696	0.539
	2	2.3	−0.559	−0.495	−0.459	–	−0.330	0.067	0.756	0.548	0.728
	3	1.2	−0.028	−0.015	0.071	–	0.840	−0.419	−0.170	0.316	0.371
Alanine-2	1	3.4	0.718	0.813	0.850	0.313	–	0.603	0.531	0.699	0.552
	2	2.2	−0.574	−0.521	−0.483	0.276	–	0.025	0.713	0.528	0.720
	3	1.1	−0.001	−0.033	−0.111	0.826	–	0.346	0.205	−0.359	−0.368
Acetate	1	5.9	0.897	0.881	0.913	0.941	0.945	–	0.851	0.633	0.790
	2	1.3	−0.392	−0.399	−0.347	−0.081	−0.090	–	0.357	0.648	0.592
Creatine	1	4.7	0.946	0.957	0.974	0.922	0.923	0.400	–	0.307	0.151
	2	1.8	−0.108	−0.049	−0.015	−0.176	−0.161	0.135	–	0.917	0.926
U4-3	1	5.3	0.928	0.924	0.940	0.959	0.956	0.342	0.730	–	0.476
	2	1.4	−0.233	−0.301	−0.259	0.075	0.060	−0.480	0.525	–	0.817
U4-4	1	5.2	0.944	0.959	0.967	0.940	0.936	0.536	0.631	0.241	–
	2	1.2	−0.030	0.052	0.037	−0.196	−0.193	0.503	−0.286	0.905	–

that include the lactate lines are given in Figs 6–9. All cases showed significant effects ($\alpha = 0.05$) under the MANOVA analysis, with most cases showing significance for both main effects and for an interaction. Formal multiple comparison analysis was not performed, but it follows from the omnibus MANOVA analysis that, as a minimum, the largest differences seen in the profile plots for the first principal components are significant when the interaction is

Table 2. Principal component directions – lactate included
l_d, line denominator; c, principal component number; λ, eigenvalue

l_d	c	λ	U1-2	U2-1	U2-2	Lactate-1	Lactate-2	Alanine-1	Alanine-2	Acetate	Creatine	U4-3	U4-4
U1-2	1	5.2	–	0.635	0.740	0.646	0.646	0.881	0.879	0.470	0.839	0.642	0.742
	2	2.4	–	0.490	0.459	−0.697	−0.708	−0.318	−0.304	0.518	−0.069	0.617	0.300
	3	1.2	–	0.483	0.377	0.126	0.144	0.033	0.057	0.375	−0.405	−0.393	−0.571
U2-1	1	4.9	0.530	–	0.618	0.783	0.783	0.930	0.924	0.013	0.827	0.385	0.655
	2	2.1	−0.035	–	0.233	−0.515	−0.533	−0.155	−0.159	0.481	0.266	0.879	0.643
	3	1.3	0.773	–	0.658	−0.209	−0.195	−0.034	−0.007	−0.114	−0.352	−0.059	−0.224
U2-2	1	4.2	0.092	−0.244	–	0.852	0.852	0.921	0.911	−0.140	0.806	0.137	0.523
	2	2.4	−0.461	−0.173	–	−0.365	−0.387	−0.096	−0.109	0.432	0.441	0.936	0.776
	3	1.1	−0.614	0.302	–	0.179	0.175	0.061	0.061	0.710	−0.030	−0.195	−0.254
Lactate-1	1	7.4	0.939	0.948	0.962	–	0.060	0.947	0.944	0.801	0.881	0.910	0.814
	2	1.3	0.146	0.141	0.116	–	0.882	0.210	0.232	−0.011	−0.339	−0.249	−0.392
Lactate-2	1	7.4	0.940	0.949	0.963	0.044	–	0.951	0.948	0.786	0.891	0.916	0.825
	2	1.2	−0.149	−0.146	−0.122	0.902	–	−0.183	−0.203	−0.010	0.306	0.186	0.347
Alanine-1	1	3.7	0.607	0.722	0.757	−0.606	−0.642	–	−0.157	0.543	0.435	0.792	0.599
	2	2.4	0.679	0.629	0.605	0.252	0.275	–	0.261	0.047	−0.580	−0.456	−0.612
	3	1.6	0.106	0.113	0.134	0.727	0.679	–	−0.358	0.245	0.596	0.051	0.234
	4	1.1	0.018	0.017	0.113	0.171	0.195	–	0.785	−0.404	−0.011	0.278	0.414
Alanine-2	1	3.8	0.635	0.741	0.775	−0.575	−0.617	0.256	–	0.562	0.471	0.784	0.597
	2	2.3	0.661	0.612	0.582	0.246	0.264	−0.156	–	0.076	−0.547	−0.485	−0.646
	3	1.8	0.082	0.073	0.083	0.736	0.688	0.509	–	0.267	0.605	0.003	0.183
Acetate	1	7.4	0.898	0.879	0.912	0.903	0.897	0.961	0.964	–	0.850	0.541	0.740
	2	1.5	−0.257	−0.257	−0.211	−0.250	−0.274	−0.041	−0.047	–	0.357	0.774	0.653
Creatine	1	5.4	0.938	0.930	0.950	0.651	0.693	0.928	0.930	0.298	–	0.115	0.023
	2	2.4	0.112	0.189	0.204	−0.613	−0.588	0.046	0.052	0.389	–	0.929	0.764
	3	1.1	−0.014	−0.082	−0.041	0.291	0.279	−0.050	−0.034	−0.723	–	0.228	0.579
U4-3	1	7.0	0.906	0.894	0.917	0.934	0.937	0.949	0.946	0.282	0.768	–	0.539
	2	1.5	0.309	0.379	0.335	−0.220	−0.203	0.028	0.041	0.541	−0.442	–	−0.756
U4-4	1	6.3	0.925	0.926	0.942	0.785	0.799	0.942	0.938	0.450	0.681	0.074	–
	2	1.9	0.177	0.254	0.228	−0.549	−0.538	0.038	0.038	0.528	−0.190	0.906	–

significant. Five of six profile plots that exclude the lactate lines and have a significant interaction term, show the maximum first principal component difference between dominant and subordinate follicles at D ≥ 17 days. The remaining case (Fig. 3) shows the maximum difference at D6W1. The maximum principal component difference between dominant and subordinate follicles all occur at D ≥ 17 days for the six profile plots that include the lactate lines and show a significant interaction. An informal inspection of the profile plots, including consideration of the second principal component, reveals a possible secondary difference contributing to the interaction at D6W1.

In all but one of the cases tested (Fig. 5*a*), there was an overall difference ($P < 0.05$) between dominant and subordinate follicles. The line ratios of follicular fluid varied with time ($P < 0.05$) in the oestrous cycle in all but four of the cases tested (Figs 7 and 9*a*,*c*).

Discussion

Significant differences between subordinate and dominant follicles at D1W2 were observed in the lactate T_1 value. We interpret this difference to mean that the levels of lactate in the follicular fluid, or at least lactate's interactions with other molecules in the follicular fluid, reflect to some degree the physiological status of the follicle. This interpretation is evident in spite of the fact that the lactate is probably produced from cell death at the time of ovariectomy. This conclusion is further supported by the MANOVA analyses of line ratio principal components that included or excluded the lactate lines, which gave similar results in each case. Since T_1 variation can be caused by changes in viscosity, we may be observing the known difference in viscosity of follicular fluid between potentially ovulatory and non-ovulatory follicles (Guraya 1985).

The dominant follicle at D ≥ 17 is known to be physiologically different from dominant follicles at the other three selected time points because it will ovulate while the dominant follicle from the first wave will become atretic if there is no intervention such as lysing the corpus luteum or the introduction of gonadotrophin-releasing hormone (GnRH) at the appropriate time. Also, all subordinate follicles are committed to atresia (Adams and Pierson 1995). The expected difference between a follicle physiologically selected for ovulation and other follicles is clearly reflected in the differences observed at D ≥ 17 between dominant and subordinate follicles in the line ratio principal component analyses. It is possible also that the observed main effects of T and S are a

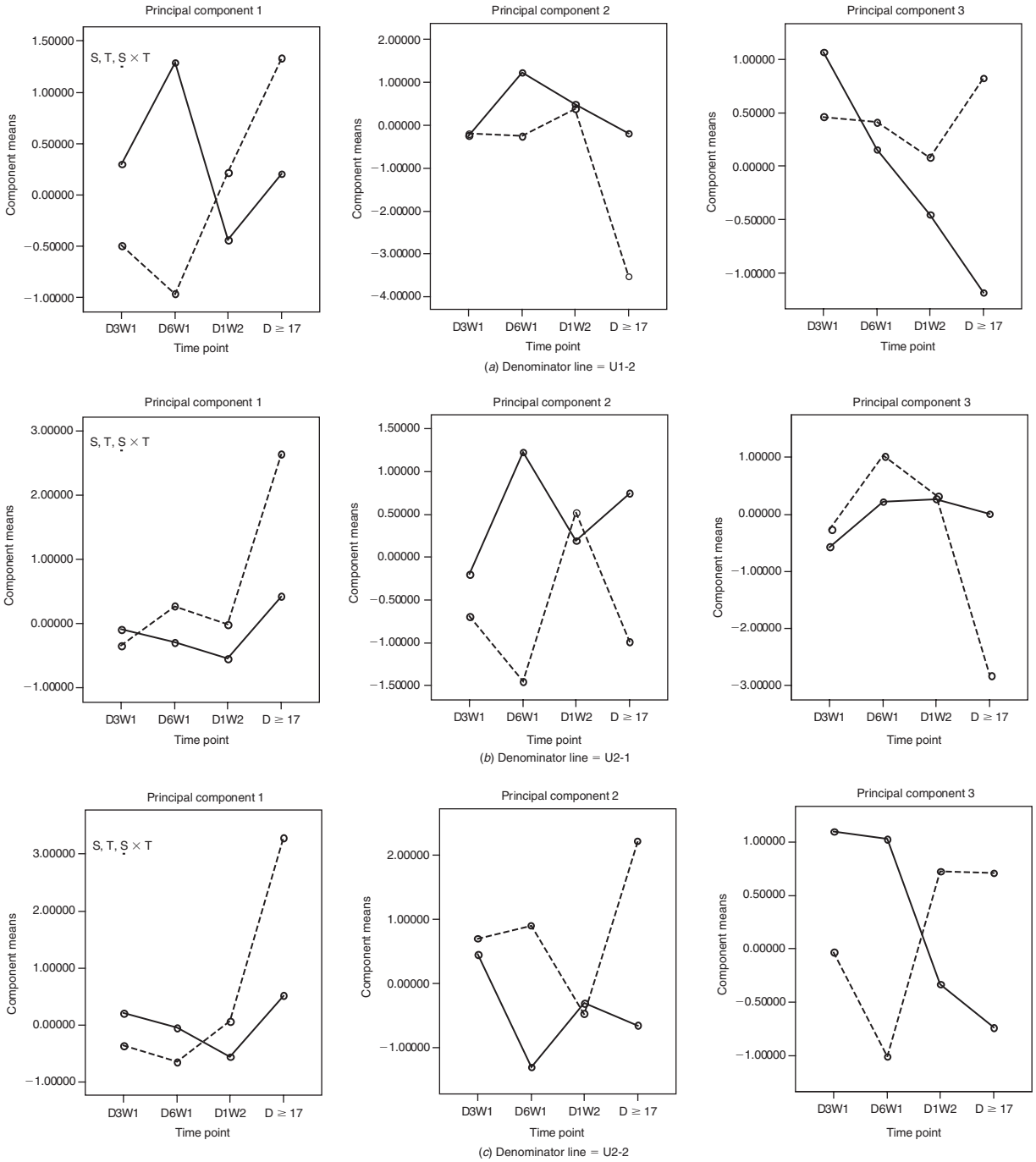

Fig. 3. Profile plots of principal components from dominant (—) and subordinate (- -) follicles – lactate not considered, denominator lines: (*a*) U1-2, $\Lambda_S = 0.341$ ($P < 0.001$), $\Lambda_T = 0.203$ ($P = 0.001$), $\Lambda_{T \times S} = 0.180$ ($P < 0.001$); (*b*) U2-1, $\Lambda_S = 0.338$ ($P < 0.001$), $\Lambda_T = 0.197$ ($P < 0.001$), $\Lambda_{T \times S} = 0.181$ ($P < 0.001$); (*c*) U2-2, $\Lambda_S = 0.327$ ($P < 0.001$), $\Lambda_T = 0.196$ ($P < 0.001$), $\Lambda_{T \times S} = 0.101$ ($P < 0.001$). Significant effects are indicated in the upper left hand corner of the profile plots of principal component 1; S = status (dominant, subordinate), T = time point (D3W1, D6W1, D1W2, D ≥ 17), S × T = status by time point interaction. Wilk's λ for the main effects of S, T and the interaction S × T are denoted by Λ_S, Λ_T and $\Lambda_{T \times S}$ respectively.

result of the large difference at D ≥ 17 between line ratios in dominant and subordinate follicles.

Our follicular fluid samples were acquired *ex vivo* after ovariectomy. Gérard *et al*. (2002) obtained small quantities of follicular fluid (small enough not to interfere with follicle maturation) for NMR analysis using *in vivo* aspiration from mares. A formic acid reference peak was used to quantify peak amplitudes directly without resorting to line ratios.

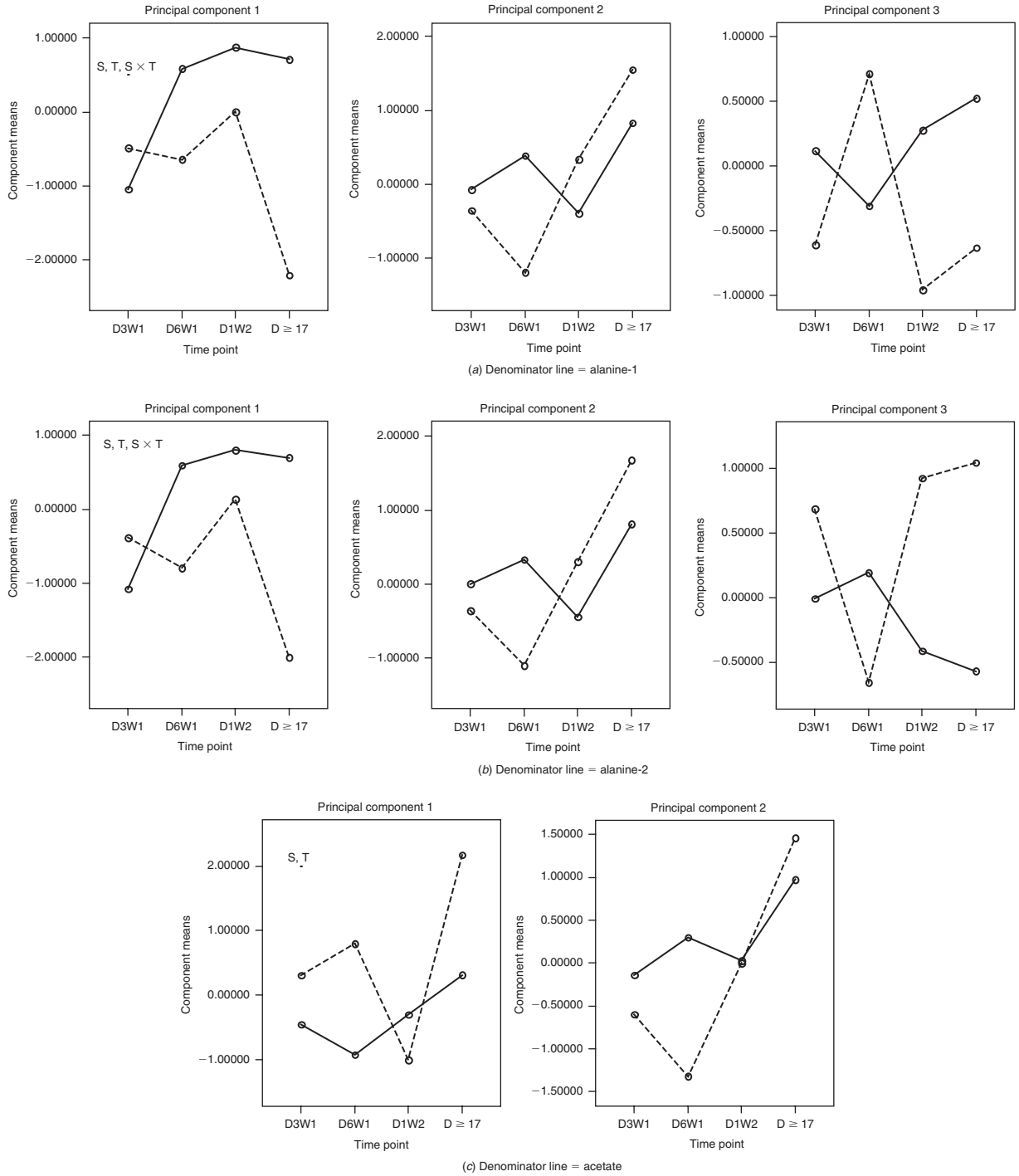

Fig. 4. Profile plots of principal components from dominant (—) and subordinate (- -) follicles – lactate not considered, denominator lines: (*a*) alanine-1, $\Lambda_S = 0.460$ ($P = 0.004$), $\Lambda_T = 0.370$ ($P = 0.032$), $\Lambda_{T \times S} = 0.297$ ($P = 0.008$); (*b*) alanine-2, $\Lambda_S = 0.466$ ($P = 0.004$), $\Lambda_T = 0.371$ ($P = 0.032$), $\Lambda_{T \times S} = 0.297$ ($P = 0.008$); (*c*) acetate, $\Lambda_S = 0.709$ ($P = 0.045$), $\Lambda_T = 0.415$ ($P = 0.011$), $\Lambda_{T \times S} = 0.563$ ($P = 0.091$). See caption of Fig. 3 for additional notes.

The mare follicles apparently grew in a single wave in one oestrous cycle and follicular fluid samples were aspirated from the dominant follicle at an early dominant stage (roughly equivalent to our dominant follicle at D3W1), a late dominant stage (roughly equivalent to our dominant follicle at D6W1) and at the preovulatory stage (roughly equivalent to our dominant follicle at D ≥ 17). The mare follicles were induced to ovulate with the injection of an exogenous gonadotrophin.

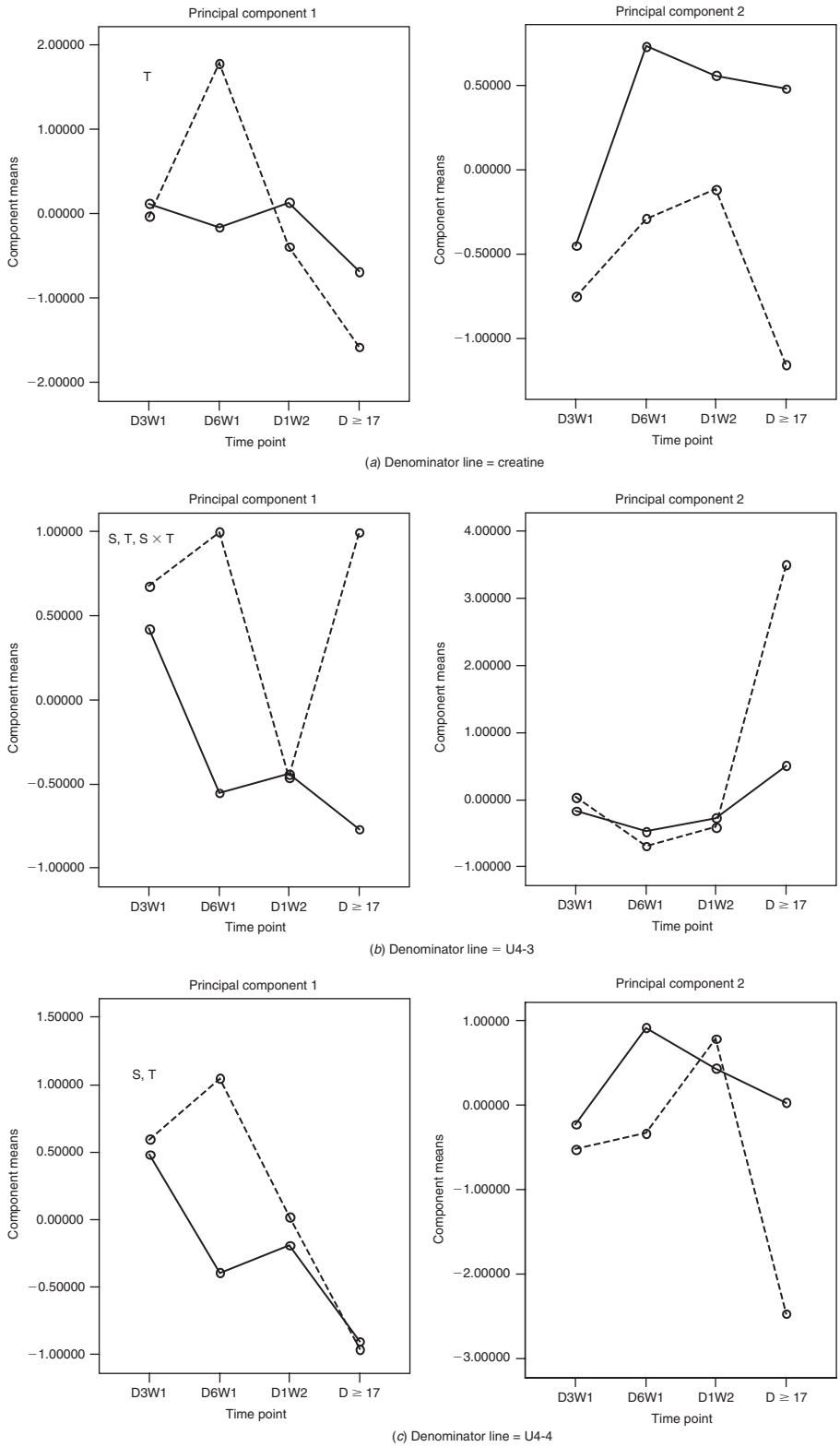

Fig. 5. Profile plots of principal components from dominant (—) and subordinate (- -) follicles – lactate not considered, denominator lines: (*a*) creatine, $\Lambda_S = 0.788$ ($P = 0.117$), $\Lambda_T = 0.489$ ($P = 0.035$), $\Lambda_{T \times S} = 0.585$ ($P = 0.117$); (*b*) U4-3, $\Lambda_S = 0.614$ ($P = 0.012$), $\Lambda_T = 0.298$ ($P = 0.001$), $\Lambda_{T \times S} = 0.478$ ($P = 0.030$); (*c*) U4-4, $\Lambda_S = 0.690$ ($P = 0.035$), $\Lambda_T = 0.458$ ($P = 0.022$), $\Lambda_{T \times S} = 0.629$ ($P = 0.186$). See caption of Fig. 3 for additional notes.

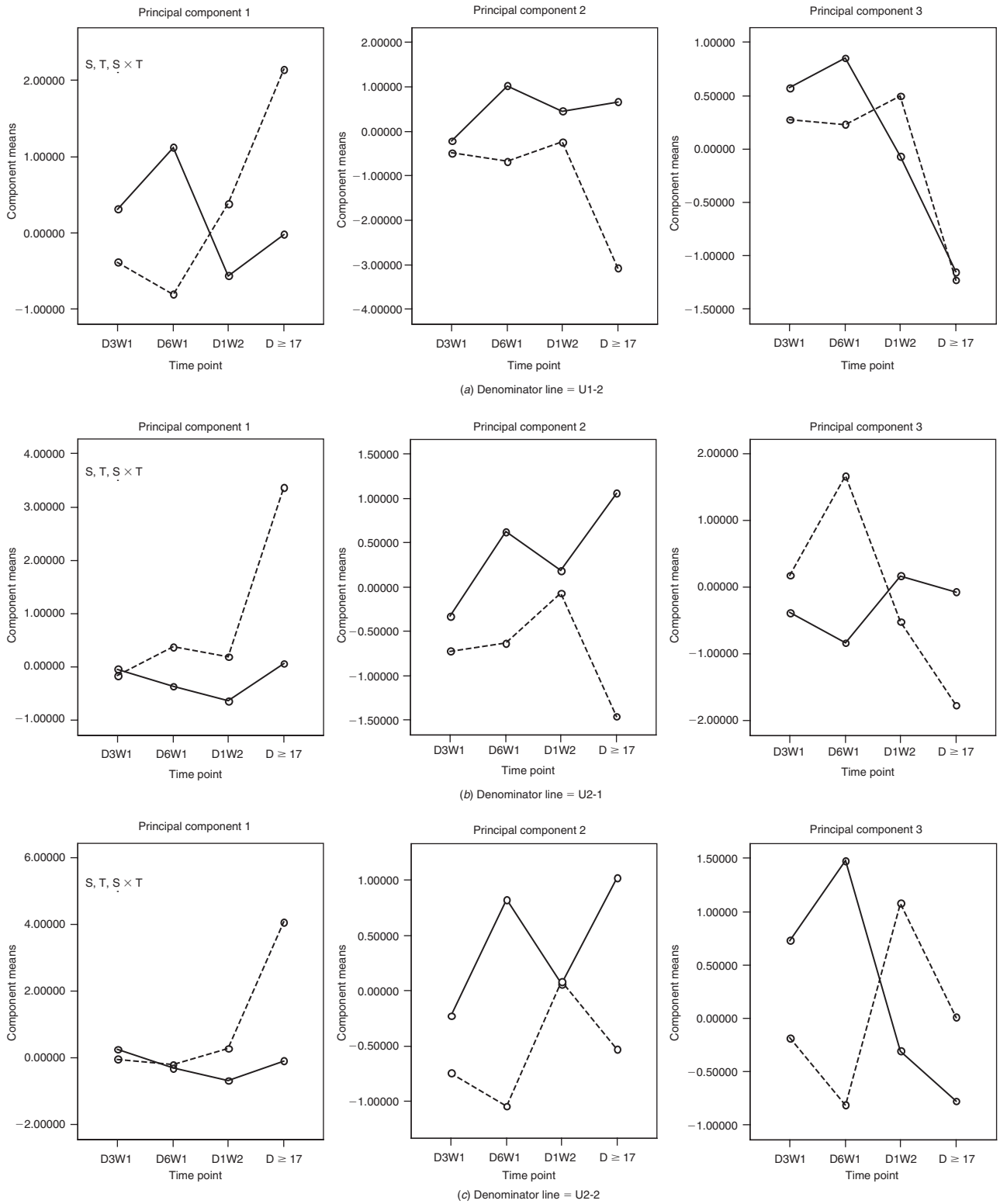

Fig. 6. Profile plots of principal components from dominant (—) and subordinate (- -) follicles – lactate included, denominator lines: (*a*) U1-2, $\Lambda_S = 0.332$ ($P < 0.001$), $\Lambda_T = 0.334$ ($P = 0.017$), $\Lambda_{T \times S} = 0.227$ ($P = 0.001$); (*b*) U2-1, $\Lambda_S = 0.312$ ($P < 0.001$), $\Lambda_T = 0.289$ ($P = 0.007$), $\Lambda_{T \times S} = 0.165$ ($P < 0.001$); (*c*) U2-2, $\Lambda_S = 0.293$ ($P < 0.001$), $\Lambda_T = 0.279$ ($P = 0.005$), $\Lambda_{T \times S} = 0.109$ ($P < 0.001$). See caption of Fig. 3 for additional notes.

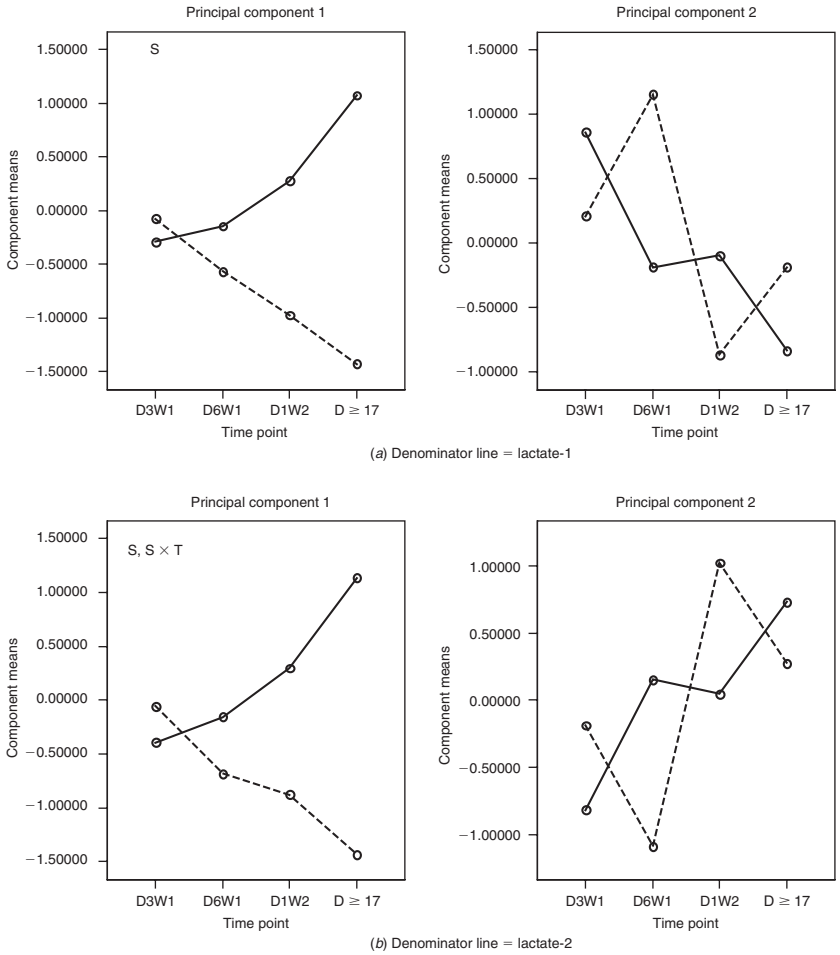

Fig. 7. Profile plots of principal components from dominant (—) and subordinate (- -) follicles – lactate included, denominator lines: (*a*) lactate-1, $\Lambda_S = 0.689$ ($P = 0.035$), $\Lambda_T = 0.690$ ($P = 0.317$), $\Lambda_{T \times S} = 0.517$ ($P = 0.052$); (*b*) lactate-2, $\Lambda_S = 0.699$ ($P = 0.040$), $\Lambda_T = 0.687$ ($P = 0.311$), $\Lambda_{T \times S} = 0.508$ ($P = 0.045$). See caption of Fig. 3 for additional notes.

The cow follicles in the present study grew in two waves through the oestrous cycle and no exogenous gonadotrophin was used.

For the mare study (Gérard *et al*. 2002), decreases in alanine and lipoproteins between the early and late dominant stages, a decrease in sugar chain amplitudes between late dominant and preovulatory stages and decreases in trimethylamine and acetate were observed between the late dominant and preovulatory stages. No observations of progesterone were reported in the mare study, whereas progesterone, or at least peaks where progesterone would be expected, was observed in some of our spectra. Making reference to the peaks observed in the mare study, we observed alanine (∼1.7 p.p.m.) but not lipoproteins (∼0.8 p.p.m.) in the NMR spectra. We also observed the sugar chain peaks but did not quantify them because their amplitudes were generally low. Finally, we observed acetate (∼1.85 p.p.m.) but not trimethylamine (∼3.2 p.p.m.). Our principal components approach to data analysis did not allow us to determine whether alanine in the dominant follicle decreased from D3W1 to D6W1 or whether acetate in the dominant follicle decreased between D6W1 and D ≥ 17 as was observed by Gérard *et al*. (2002); we can only report that the amount of both alanine and acetate were significantly different between dominant and subordinate follicles at D ≥ 17 because they are dominantly represented in most first principal components (Tables 1 and 2).

Nuclear magnetic resonance spectroscopy of ovarian follicular fluid can be used to detect changes that may be used to differentiate dominant and subordinate follicles. It follows that viable or non-viable follicles that develop under ovarian super stimulation protocols may also be detected using this technologic approach to understanding follicular function. Further exploration of NMR spectra is well justified in

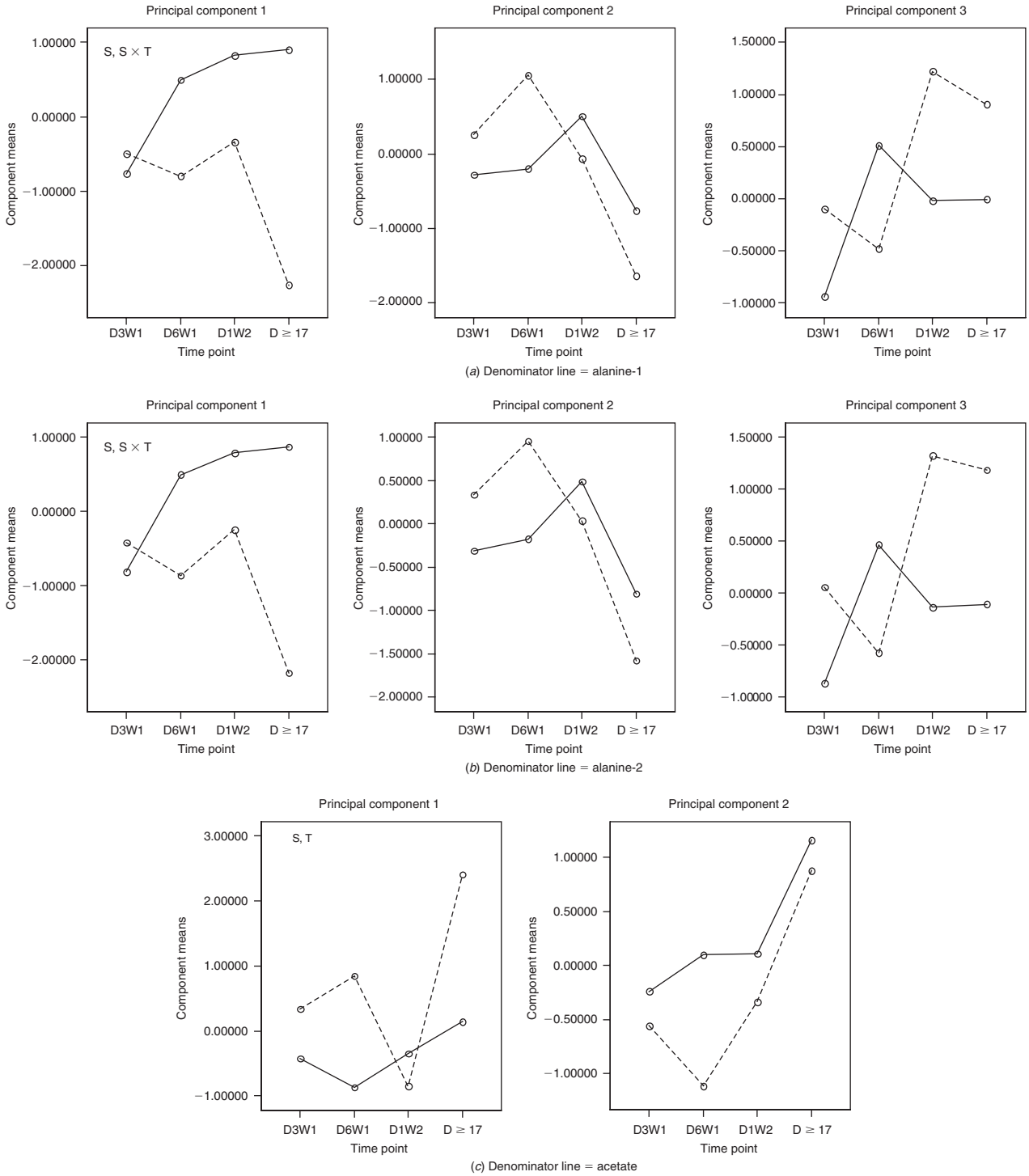

Fig. 8. Profile plots of principal components from dominant (—) and subordinate (- -) follicles – lactate included, denominator lines: (*a*) alanine-1, $\Lambda_S = 0.386$ ($P = 0.003$), $\Lambda_T = 0.356$ ($P = 0.102$), $\Lambda_{T \times S} = 0.268$ ($P = 0.024$), component 4 ($\lambda = 1.1$) not shown; (*b*) alanine-2, $\Lambda_S = 0.473$ ($P = 0.004$), $\Lambda_T = 0.438$ ($P = 0.085$), $\Lambda_{T \times S} = 0.338$ ($P = 0.018$); (*c*) acetate, $\Lambda_S = 0.622$ ($P = 0.014$), $\Lambda_T = 0.465$ ($P = 0.024$), $\Lambda_{T \times S} = 0.656$ ($P = 0.238$). See caption of Fig. 3 for additional notes.

experiments to understand follicular physiology during ovarian stimulation protocols. The bovine model will provide an excellent model for understanding the physiological status and oocyte competence and may help to assess the probability of conception during ART cycles. If the concepts of differential expression of NMR detectable variables are validated in the bovine model, a study on human follicular fluid aspirated at oocyte retrieval for ART may be warranted.

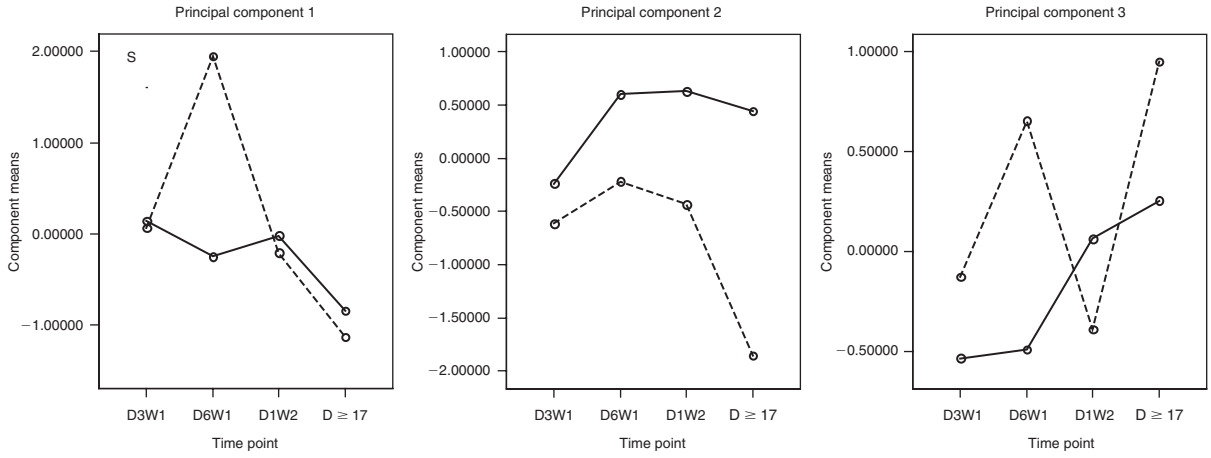

(*a*) Denominator line = creatine

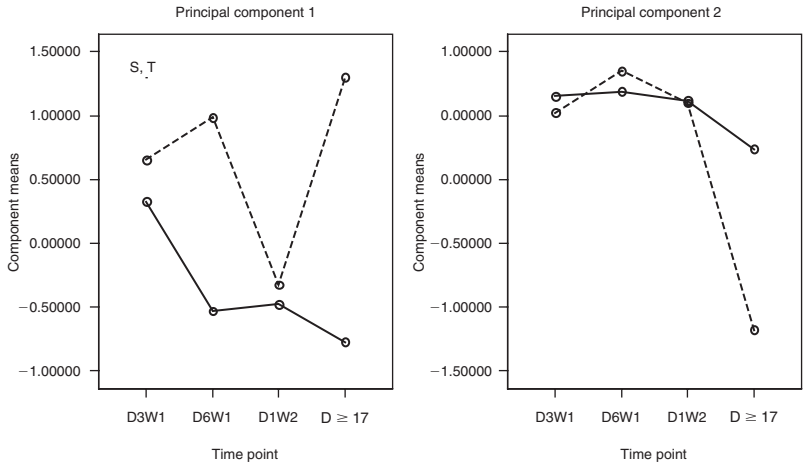

(*b*) Denominator line = U4-3

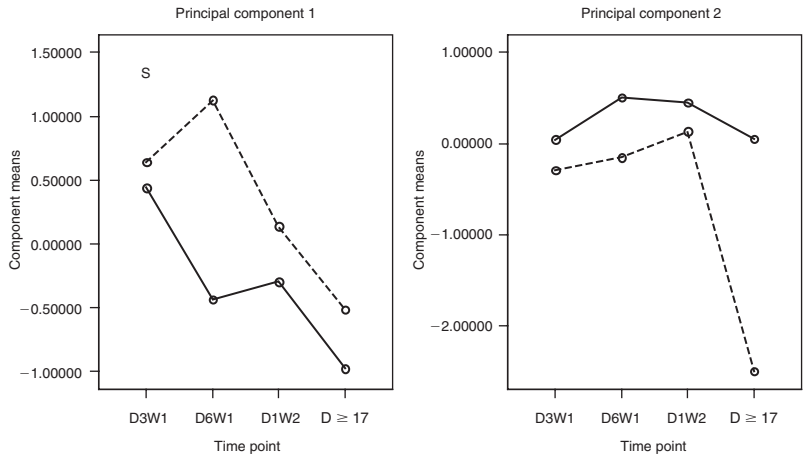

(*c*) Denominator line = U4-4

Fig. 9. Profile plots of principal components from dominant (—) and subordinate (- -) follicles – lactate included, denominator lines: (*a*) creatine, $\Lambda_S = 0.594$ ($P = 0.28$), $\Lambda_T = 0.465$ ($P = 0.118$), $\Lambda_{T \times S} = 0.479$ ($P = 0.138$); (*b*) U4–3, $\Lambda_S = 0.593$ ($P = 0.009$), $\Lambda_T = 0.351$ ($P = 0.003$), $\Lambda_{T \times S} = 0.524$ ($P = 0.057$); (*c*) U4–4, $\Lambda_S = 0.668$ ($P = 0.027$), $\Lambda_T = 0.600$ ($P = 0.139$), $\Lambda_{T \times S} = 0.743$ ($P = 0.465$). See caption of Fig. 3 for additional notes.

Acknowledgments

Funding for this project was provided by the Canadian Institute for Health Research (CIHR) and the Natural Sciences and Engineering Research Council (NSERC) of Canada. Thanks are given to Jennifer Hadley who quantified the spectral data before statistical analysis.

References

Adams, G. P., and Pierson, R. A. (1995). Bovine model for the study of ovarian follicular dynamics in humans. *Theriogenology* **43**, 113–121. doi:10.1016/0093-691X(94)00015-M

Baerwald, A. R., Adams, G. P., and Pierson, R. A. (2003*a*). A new model for folliculogenesis during the menstrual cycle in women. *Fertil. Steril.* **80**, 116–122. doi:10.1016/S0015-0282(03)00544-2

Baerwald, A. R., Adams, G. P., and Pierson, R. A. (2003*b*). Characterization of ovarian follicular wave dynamics in women. *Biol. Reprod.* **69**, 1023–1031. doi:10.1095/BIOLREPROD.103.017772

Gérard, N., Loiseau, S., Duchamp, G., and Seguin, F. (2002). Analysis of the variations of follicular fluid composition during follicular growth and maturation in the mare using proton nuclear magnetic resonance (^{1}H NMR). *Reproduction* **124**, 241–248. doi:10.1530/REP.0.1240241

Ginther, O. J., Gastal, E. L., Gastal, M. O., Bergfelt, D. R., Baerwald, A. R., and Pierson, R. A. (2004). Comparative study of the dynamics of follicular waves in mares and women. *Biol. Reprod.* **71**, 1195–1201. doi:10.1095/BIOLREPROD.104.031054

Guraya, S. S. (1985). 'Biology of Ovarian Follicles in Mammals.' (Springer-Verlag: Berlin, Germany.)

Hilton, J. L., Sarty, G. E., Adams, G. P., and Pierson, R. A. (2000). Magnetic resonance image attributes of the bovine ovarian follicle antrum during development and regression. *J. Reprod. Fertil.* **120**, 311–323. doi:10.1530/REPROD/120.2.311

Hilton, J. L., Sarty, G. E., Adams, G. P., and Pierson, R. A. (2001). Magnetic resonance image attributes of the ovarian follicle wall during development and regression. *Biol. Reprod.* **65**, 1067–1073. doi:10.1095/BIOLREPROD65.4.1067

Hilton, J. L., Baerwald, A. R., Sarty, G. E., Adams, G. P., and Pierson, R. A. (2003). Magnetic resonance image attributes of the corpus luteum during development and regression. *Anat. Rec.* **272A**, 454–459. doi:10.1002/AR.A.10050

Hudson, R. (1986). Genital surgery of the cow. In 'Current Therapy in Theriogenology'. 2nd edn. (Ed. D. Morrow.) pp. 341–352. (WB Sanders: Toronto, Canada.)

Pretsch, E., Buhlmann, P., and Affolter, C. (2000). 'Structure Determination of Organic Compounds: Tables of Spectral Data.' (Springer: New York, USA.)

Rencher, A. C. (1998). 'Multivariate Statistical Inference and Applications.' (Wiley-Interscience: New York, USA.)

Singh, J., Pierson, R. A., and Adams, G. P. (1997). Ultrasound image attributes of the bovine corpus luteum: structural and functional correlates. *J. Reprod. Fertil.* **109**, 35–44.

Manuscript received 9 February 2006; revised and accepted 15 March 2006.